THE JOURNAL OF PHYSICAL CHEMISTRY Letters

pubs.acs.org/JPCL Letter

Confinement-Induced Enhancement of Parallel Dielectric Permittivity: Super Permittivity Under Extreme Confinement

Mohammad H. Motevaselian and Narayana R. Aluru*

Cite This: J. Phys. Chem. Lett. 2020, 11, 10532–10537 Read Online

ACCESS | Metrics & More | Article Recommendations | Supporting Information

ABSTRACT: Enhancement of parallel ($x-y$ plane) dielectric permittivity of confined fluids has been shown previously. However, a theoretical model that explains this enhancement is lacking thus far. In this study, using statistical-mechanical theories and molecular dynamics simulations, we show an explicit relation between the parallel dielectric permittivity, density variations, and dipolar correlations for protic and aprotic fluids confined in slit-like channels. We analyze the importance of dipolar correlations on enhancement of parallel dielectric permittivity inside large channels and extreme confinements. In large channels, beyond the interfacial region, dipolar correlations exhibit bulk-like behavior. Under extreme confinement, the correlations become stronger to the extent that they give rise to a giant increase in the parallel dielectric permittivity. This sudden increase in dielectric permittivity can be a signature of a liquid transition into higher-ordered structures and has important consequences for understanding ion transport, molecular dissociation, and chemical reactions inside nanoconfined environments.

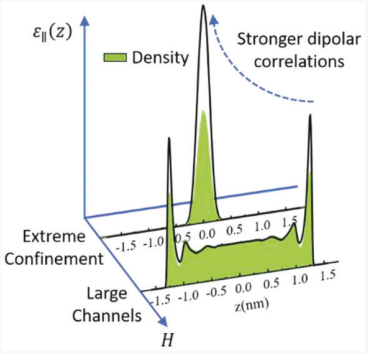

It is well-established that the properties of fluids confined in nano spaces are very different from those in bulk: density variations,[1] unusually high-pressure regions,[2,3] dynamical anomalies,[4−7] existence of different phases,[8,9] to name a few. Another example is the dielectric permittivity. Dielectric permittivity plays a crucial role in many fields of science and technology such as in electric double-layer capacitors (EDLCs),[10,11] coordination chemistry,[12] determining high-pressure hydrogen structures,[13] nanofluidics,[14] molecular transport through membranes,[15] and biophysics.[16] Unlike in bulk, the dielectric response of fluids under confinement is neither isotropic nor scalar. Dielectric permittivity is a two-rank tensor, whose components vary in different spatial directions and exhibit an anisotropic behavior. For example, next to a flat surface, the relevant components are the perpendicular to the surface, $\varepsilon_{\perp}$, and parallel to the surface, $\varepsilon_{\parallel}$, dielectric permittivity.[17−20] Understanding the anisotropic behavior is important since different applications require the use of a specific component of the dielectric permittivity tensor. For example, determining the capacitance of EDLCs requires the knowledge of perpendicular dielectric permittivity.[21] Other applications such as in nanofiltration and water desalination,[22,23] where the transport of the species is mainly parallel to the pore surface, the parallel component of the dielectric permittivity becomes the most relevant quantity. From both molecular dynamics (MD) simulations and experiments, there has been a surge of interest in studying the dielectric permittivity of confined fluids, in particular, water. Most of these efforts have focused on the perpendicular dielectric permittivity. It has been shown that the perpendicular dielectric permittivity is significantly reduced near the interface[24,25] and the reduction is universal for both protic and aprotic fluids.[26] On the other hand, the parallel dielectric permittivity is enhanced near the interface and shown to approximately follow the density variation inside the confinement.[18] It has also been shown that for water inside carbon nanotubes the axial dielectric permittivity enhances significantly as the diameter decreases.[27] The results reported from the MD simulations are primarily on confined water, and the relation between the parallel permittivity and density profile has not been rigorously established.[28,29] The molecular origin of the enhancement of parallel permittivity has been investigated for water and shown to be associated with excluded volume and hydrogen bonding network.[28,30] However, this remains an open question, when it comes to aprotic fluids as they are incapable of forming hydrogen bonds.

In this paper, we use extensive MD simulations with a cumulative time of 1 μs to study parallel permittivity variation of both protic and aprotic fluids confined in 2D graphene slit-like channels. Starting from the fluctuation formula and using statistical mechanics, we show that in addition to the density variation, dipolar correlations at the interface play an important role in enhancing the parallel dielectric permittivity depending on the fluid polarity and the degree of confinement. We also

Received: October 24, 2020
Accepted: December 1, 2020
Published: December 8, 2020

https://dx.doi.org/10.1021/acs.jpclett.0c03219
J. Phys. Chem. Lett. 2020, 11, 10532−10537

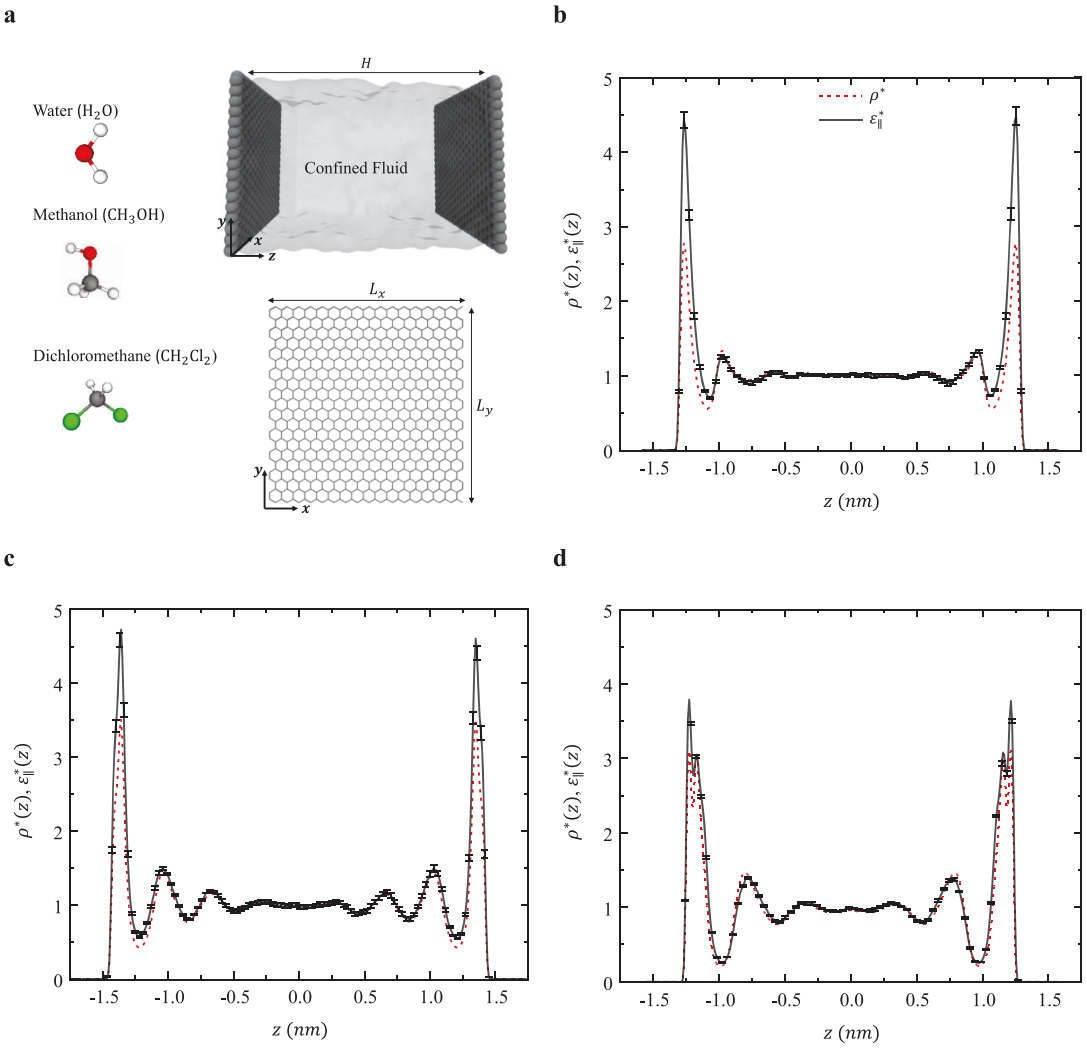

Figure 1. (a) Schematic illustration of the confined fluid between two graphene sheets separated by a distance H in the z direction. Lateral dimensions in the x and y directions are denoted by L_x and L_y, respectively. Oxygen (O, red), hydrogen (H, white), carbon (C, gray), and chloride (Cl, green) atoms are shown. Normalized parallel dielectric permittivity ($\varepsilon_\parallel^*(z) = \frac{\varepsilon_\parallel(z)-1}{\varepsilon_b-1}$) and density ($\rho^* = \frac{\rho(z)}{\rho_b}$) of confined fluids: (b) water (H = 3.17 nm), (c) methanol (H = 3.5 nm), and (d) dichloromethane (H = 3.15 nm).

elucidate the molecular origin for the enhancement of parallel permittivity. Finally, we study the parallel dielectric permittivity inside an extreme confinement, where only a single layer of fluid could fit inside the channel. We show that such confined geometries can give rise to a giant increase in parallel dielectric permittivity, which could serve as a probe to identify fluid transition into a highly ordered structure.

We simulate both protic (water and methanol) and aprotic (dichloromethane) fluids confined between two frozen graphene sheets separated by a distance H and a surface area denoted by A. A snapshot illustrating the model system is presented in Figure 1a. All simulations are carried out in the canonical ensemble (NVT) at 298 K with a time step of 1 fs using the GROMACS software.[31] Periodic boundary conditions were applied in all the directions with an extra vacuum of length at least $3H$ in the z direction. The short-ranged interactions are modeled using the standard 12−6 Lennard-Jones potential function. For the long-ranged Coulombic interactions, the common choices for a slab geometry are the Ewald algorithm[32,33] in all the directions (Ewald3d) or its slab-adapted version (Ewald3dc),[34] which excludes the long-ranged electrostatic contributions from the periodic image cells in the z direction. It has been shown that, depending on using Ewald3d or Ewald3dc, the fluctuation formula to calculate the perpendicular permittivity is different (see the Supporting Information of ref 26). For a system periodic in two dimensions and finite in the third (e.g., slit-like channels), the more efficient and accurate method is the Ewald3dc. Therefore, we choose the Ewald3dc algorithm to compute the electrostatic interactions (see the Supporting Information for more details regarding the MD simulations and force fields). For systems where the inhomogeneity is only in one direction (perpendicular to the surface, z axis), using statistical mechanics and linear response theory the locally varying parallel dielectric permittivity is given via the fluctuation formula,[17]

$$\varepsilon_\parallel(z) = 1 + \frac{\beta\varepsilon_0^{-1}}{2}[\langle \mathbf{p}_\parallel(z)\cdot\mathbf{P}_\parallel\rangle_0 - \langle \mathbf{p}_\parallel(z)\rangle_0\cdot\langle \mathbf{P}_\parallel\rangle_0] \quad (1)$$

https://dx.doi.org/10.1021/acs.jpclett.0c03219
J. Phys. Chem. Lett. 2020, 11, 10532−10537

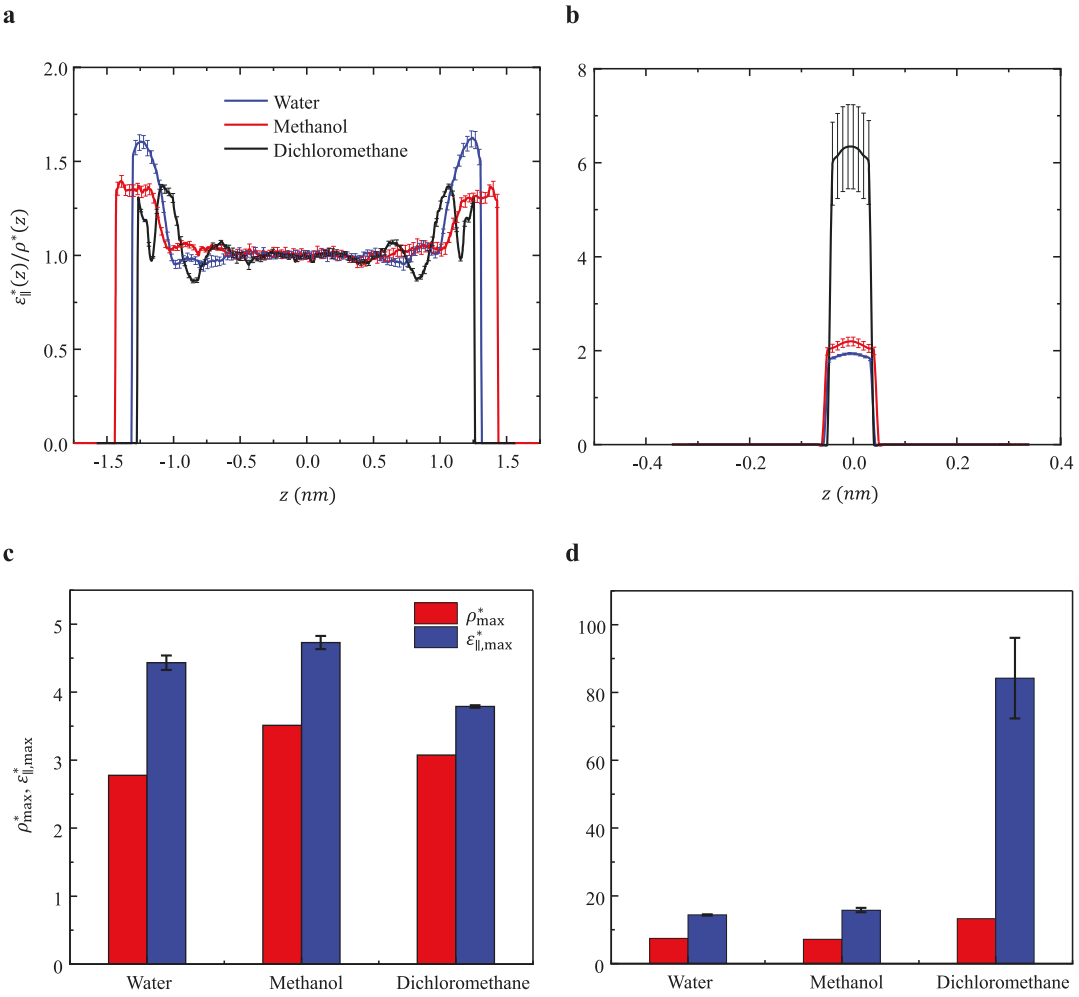

Figure 2. Normalized space-dependent parallel dipolar correlations of water, methanol, and dichloromethane inside (a) large channels and (b) under extreme confinement. The normalized correlations are obtained from eq 9 by calculating the ratio, $\varepsilon^*_{\parallel}(z)/\rho^*_{\parallel}(z)$. The bottom row shows the histograms of maximum normalized density and parallel permittivity for (c) large channels and (d) extreme confinements.

where $\beta = 1/k_B T$ with k_B as the Boltzmann constant and T as the temperature, ε_0 is the vacuum permittivity, $\langle \cdots \rangle_0$ denotes the ensemble average in the absence of an external electric field, $\mathbf{p}_{\parallel} = (p_x, p_y)$ is the in-plane fluid polarization density vector at position z, and $\mathbf{P}_{\parallel}$ is the parallel component of the fluid total polarization vector. It has been shown that for confined water, higher-order multipole moments such as quadrupole and octupole are negligible in calculating the parallel dielectric permittivity.[18] To verify this for other confined fluids, in addition to water, we calculate the parallel dielectric permittivity of methanol and dichloromethane using all the multipole moments. As shown in Figure S2, the higher-order multipole moments beyond the dipole have a negligible effect on the parallel dielectric permittivity of confined polar fluids. Therefore, the total parallel polarization and the local parallel polarization density calculated from MD can be written in terms of the molecular dipole moment,

$$\mathbf{P}_{\parallel} = \sum_{j=1}^{N} \boldsymbol{\mu}_{\parallel,j} \tag{2}$$

$$\mathbf{p}_{\parallel}(z_i) = \frac{1}{A\Delta z} \sum_{j=1}^{N(z_i)} \boldsymbol{\mu}_{\parallel,j} \tag{3}$$

where $\boldsymbol{\mu}_{\parallel,j} = (\mu_{x,j}, \mu_{y,j})$ is the parallel component of the jth dipole, A is the surface area of graphene, N is the total number of fluid molecules, $N(z_i)$ represents the number of molecules located at $z = z_i$, and z_i is the location of the ith layer (bin) of thickness Δz inside the slit channel. Due to the homogeneity in the $x-y$ plane, the contribution of $\langle \mathbf{p}_{\parallel}(z) \rangle_0 \cdot \langle \mathbf{P}_{\parallel} \rangle_0$ in eq 1 is negligible. Therefore, using definitions provided in eqs 2 and 3, we arrive at

$$\varepsilon_{\parallel}(z_i) = 1 + \frac{\beta \varepsilon_0^{-1}}{2A\Delta z} \left[\sum_{j=1}^{N(z_i)} \langle \mu_{\parallel,j}^{\ 2} \rangle + \sum_{j=1}^{N(z_i)} \sum_{k \neq j}^{N} \langle \boldsymbol{\mu}_{\parallel,j} \cdot \boldsymbol{\mu}_{\parallel,k} \rangle \right] \tag{4}$$

In eq 4, the first summation is the dipole−dipole self-correlation within a layer and the second summation is the cross-correlation between dipoles of the ith layer and the entire system. We can further rewrite eq 4 as

https://dx.doi.org/10.1021/acs.jpclett.0c03219
J. Phys. Chem. Lett. 2020, 11, 10532−10537

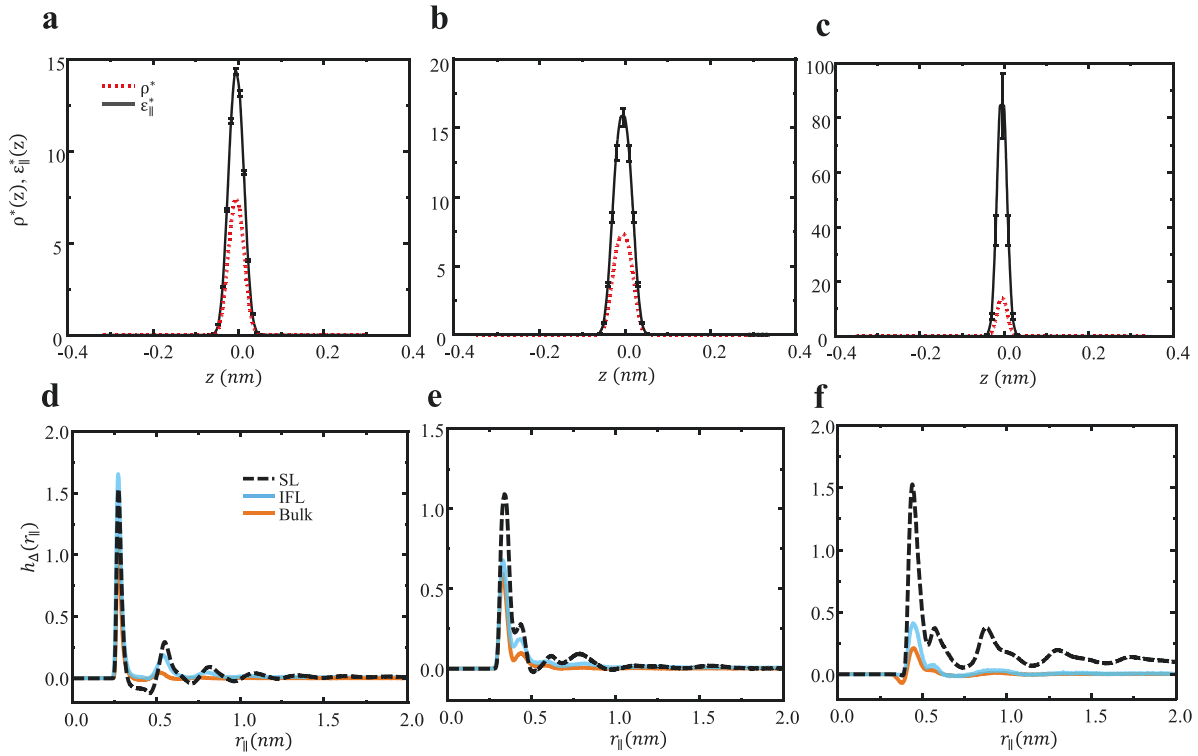

Figure 3. (a)−(c) Normalized density and parallel permittivity distribution of water (a), methanol (b), and dichloromethane (c) under an extreme confinement (single-layer density). Dipole−dipole in-plane pair correlation functions of bulk, IFL, and confined single-layer (SL) water, methanol, and dichloromethane depicted in subplots d−f, respectively. It is important to note that in extreme confinement the distance between the dipoles lies in the *xy* plane (parallel to the surface). Therefore, the separation distance is the in-plane radial distance, i.e., $\mathbf{r}_{\parallel} = (x, y)$.

$$\varepsilon_{\parallel}(z_i) = 1 + \frac{\rho(z_i)\langle \mu_{\parallel}^{\,2}\rangle}{2\varepsilon_0 k_B T}\left(1 + \int \rho(z_i)\, h_{\Delta}(r, z_i)\, \mathrm{d}\mathbf{r}\right) \tag{5}$$

where $\rho(z_i)$ is the density at location z_i, $\mathbf{r}$ is the radial distance vector with magnitude r, and $h_{\Delta}(r, z_i)$ is the z-dependent parallel dipole−dipole correlation function and is defined as

$$h_{\Delta}(r, z_i) = \frac{1}{N(z_i)\,\rho(z_i)}\left\langle \sum_{j=1}^{N(z_i)} \sum_{k\neq j}^{N} \hat{\boldsymbol{\mu}}_{\parallel,j} \cdot \hat{\boldsymbol{\mu}}_{\parallel,k}\, \delta(\mathbf{r} - \mathbf{r}_{jk}) \right\rangle \tag{6}$$

where $\mathbf{r}_{jk} = \mathbf{r}_j - \mathbf{r}_k$ is the center-to-center distance between j and k dipoles and $\hat{\boldsymbol{\mu}}_{\parallel}$ is the unit vector in the direction of $\boldsymbol{\mu}_{\parallel}$. The term in the parentheses in eq 5 accounts for angular correlations among the dipoles and is similar to the definition of the well-known Kirkwood g factor in the bulk, i.e., $G_{k,b}$.[35,36] Thus, we recast eq 5 in terms of the z-dependent Kirkwood g factor, $G_k(z)$:

$$\varepsilon_{\parallel}(z) = 1 + \frac{\rho(z)\langle \mu_{\parallel}^{\,2}\rangle}{2\varepsilon_0 k_B T} G_k(z) \tag{7}$$

Equation 7 explicitly shows the relation between the parallel dielectric permittivity, density variations, and angular correlations inside slit-like confinement. On the other hand, for a homogeneous system (bulk) of polar molecules with periodic boundary conditions, the bulk dielectric permittivity is calculated from the following relation:

$$\varepsilon_b = 1 + \frac{\rho_b \langle \mu^2\rangle G_{k,b}}{3\varepsilon_0 k_B T} \tag{8}$$

with ρ_b representing the bulk density. Combining eqs 7 and 8 yields

$$\varepsilon_{\parallel}^{*}(z) = \frac{3}{2}\rho^{*}(z)\frac{\langle \mu_{\parallel}^{\,2}\rangle G_k(z)}{\langle \mu^2\rangle G_{k,b}} \tag{9}$$

where $\varepsilon_{\parallel}^{*} = \frac{\varepsilon_{\parallel}(z) - 1}{\varepsilon_b - 1}$ is the normalized parallel permittivity and $\rho^{*} = \frac{\rho(z)}{\rho_b}$ is the normalized density.

Panels b−d of Figure 1 show the variation of the normalized parallel dielectric permittivity and density profile inside the confined nano channels with a well-defined bulk region (large channels). For all the fluids considered, beyond the first fluid density layer (interfacial layer (IFL)), $\varepsilon_{\parallel}^{*}$ closely follows the density variation inside the channel. This indicates that except for the interfacial region, the dipolar angular correlations in confinement behave similarly to that of the bulk regardless of the proticity of the fluid (see Figure 2a). In the interfacial region, however, depending on the type of the fluid, the dipolar correlations deviate from the bulk and contribute to the enhancement of the parallel dielectric permittivity. Figure 2c shows the contribution of density to the interfacial parallel dielectric permittivity. For protic and more polar fluids such as water and methanol, in addition to density, dipolar correlations are also responsible for enhancing the parallel dielectric permittivity adjacent to the wall. For dichloromethane, a less polar and aprotic fluid, dipolar correlations have a smaller contribution in enhancing the parallel dielectric permittivity compared to the high-density region in the IFL. Thus, for fluids such as dichloromethane, with a good approximation, the

https://dx.doi.org/10.1021/acs.jpclett.0c03219
J. Phys. Chem. Lett. 2020, 11, 10532−10537

parallel permittivity in larger channels, where confinement effects are not significant, can be obtained from the density variations (see Figure 1d). We have also calculated the in-plane dipolar correlation in the IFL (i.e., $h_{\Delta}(r_{\parallel})$ from eq 6 with N replaced by $N(z_{IFL})$ and $\mathbf{r}_{\parallel} = (x, y)$) to investigate the effect of interface on the planar dipolar correlation. A closer look at Figure 3d−f reveals a higher in-plane dipolar correlation in IFL for more protic and polar fluids (water > methanol > dichloromethane). This not only corroborates the notion that the hydrogen bonding network increases the parallel dielectric permittivity[30,37] but also reveals a deeper underlying explanation for enhancement of parallel dielectric permittivity, which is the preferred alignment of the dipoles parallel to the graphene sheet (see the Supporting Information for orientational profiles and angle distributions, Figures S3 and S4).

As shown in Figure 3a−c, we also study fluids under extreme confinement characterized by a single-layer density (SL). Due to the degree of confinement, the fluid molecules arrange in a condensed single-layer sheet creating a high-density layer with a more ordered in-plane structure compared to the bulk (see the Supporting Information, Figure S6). We observe large enhancement factors of ∼15, 16, and 85 in the parallel dielectric response of water, methanol, and dichloromethane, respectively, compared to their bulk dielectric constant. Due to the single-layer arrangement, the relevant angular correlation is the in-plane parallel dipole−dipole correlation. Looking at Figure 2b, it appears that the role of in-plane dipolar correlation becomes more prominent when fluid molecules acquire a single-layer arrangement. The dipolar correlation analysis shows that extreme confinement enhances the in-plane dipolar correlations (see Figure 3d−f), to the extent that an aprotic, less polar molecule, such as dichloromethane exhibits an abnormally large parallel dielectric permittivity of 85 times higher than its bulk dielectric constant. In such confinement, the density enhancement over the bulk contributes only ∼15% to the normalized parallel dielectric permittivity of dichloromethane, whereas for dichloromethane confined in the large slit channel this contribution in the IFL is ∼86% (see Figure 2c,d). This finding is in contrast to what has been reported in the literature for fluids confined in large channels, wherein the density variations are the dominant factor in enhancing the parallel dielectric permittivity.[18,21] The role of in-plane dipolar correlation is more evident in Figure 3d−f, where the correlations exhibit more oscillations and higher peaks compared to the bulk and IFL in-plane angular correlations. It can be seen that, although the layer thickness is approximately the same, the nature of the fluid in IFL inside large channels is very different from the fluid layer in extreme confinement. Thus, the dipolar prealignment parallel to the surface and ordered structural arrangement result in super permittivity inside extreme nanoconfinement (see the Supporting Information, Figures S7 and S8). Such an abnormal enhancement can be utilized to identify the onset of liquid transition into higher-ordered structures. High dielectric permittivity has also been found to significantly affect water self-dissociation next to graphene surfaces.[38,39] Moreover, high values of permittivity can stabilize electrochemical reactions between charge species.[40] Therefore, this opens up opportunities to effectively host highly charged and polarized species by using extreme confinement.

In summary, using statistical mechanics and MD simulations, we show that both a high-density layer and dipolar correlations are responsible for the enhancement of the parallel dielectric permittivity in the interfacial region. To what extent they affect the permittivity depends on the fluid polarity, proticity, and the degree of confinement. We show that beyond the interfacial region, protic and aprotic fluids exhibit bulk-like dipolar correlations. Our results reveal that under extreme confinement the dipole−dipole correlation becomes stronger and a single-layer arrangement of molecules can lead to large values of parallel dielectric permittivity in graphene slit-like channels. We believe that such high values of permittivity can be utilized to identify the onset of liquid transition to higher-ordered structures and possibly phase transition.

■ ASSOCIATED CONTENT

Supporting Information

The Supporting Information is available free of charge at https://pubs.acs.org/doi/10.1021/acs.jpclett.0c03219.

MD computational details and force fields, figure showing the parallel dielectric permittivity of water, effect of higher-order moments on the parallel dielectric permittivity, orientation profiles and angular distributions, density profiles, in-plane radial distribution function, and contour plot of the COM of dichloromethane molecules(PDF)

■ AUTHOR INFORMATION

Corresponding Author

Narayana R. Aluru − *Department of Mechanical Science and Engineering, University of Illinois at Urbana−Champaign, Urbana, Illinois 61801, United States;* orcid.org/0000-0002-9622-7837; Email: aluru@illinois.edu

Author

Mohammad H. Motevaselian − *Department of Mechanical Science and Engineering, University of Illinois at Urbana−Champaign, Urbana, Illinois 61801, United States;* orcid.org/0000-0002-0728-2966

Complete contact information is available at: https://pubs.acs.org/10.1021/acs.jpclett.0c03219

Notes

The authors declare no competing financial interest.

■ ACKNOWLEDGMENTS

The work on parallel permittivity of water was supported by the Center for Enhanced Nanofluidic Transport (CENT), an Energy Frontier Research Center funded by the U.S. Department of Energy, Office of Science, Basic Energy Sciences (Award # DE-SC0019112). The other aspects of this work are supported by the National Science Foundation under Grants 1545907, 1708852, 1720633, and 1921578. The computing power is provided by the Extreme Science and Engineering Discovery Environment (XSEDE) granted by National Science Foundation (NSF) Grant No. OCI1053575 and Blue Waters supercomputing center, awarded by the state of Illinois and NSF, OCI-0725070, ACI-1238993.

■ REFERENCES

(1) Ruiz-Barragan, S.; Muñoz-Santiburcio, D.; Marx, D. Nanoconfined Water within Graphene Slit Pores Adopts Distinct Confinement-Dependent Regimes. *J. Phys. Chem. Lett.* **2019**, *10*, 329−334.

(2) Long, Y.; Palmer, J. C.; Coasne, B.; Śliwinska-Bartkowiak, M.; Gubbins, K. E. Pressure Enhancement in Carbon Nanopores: A Major Confinement Effect. *Phys. Chem. Chem. Phys.* **2011**, *13*, 17163−17170.
(3) Motevaselian, M. H.; Aluru, N. R. An EQT-Based CDFT Approach for Thermodynamic Properties of Confined Fluid Mixtures. *J. Chem. Phys.* **2017**, *146*, 154102.
(4) Holt, J. K.; Park, H. G.; Wang, Y.; Stadermann, M.; Artyukhin, A. B.; Grigoropoulos, C. P.; Noy, A.; Bakajin, O. Fast Mass Transport through Sub-2-Nanometer Carbon Nanotubes. *Science* **2006**, *312*, 1034−1037.
(5) Joseph, S.; Aluru, N. R. Why Are Carbon Nanotubes Fast Transporters of Water? *Nano Lett.* **2008**, *8*, 452−458.
(6) Suk, M. E.; Aluru, N. R. Water Transport through Ultrathin Graphene. *J. Phys. Chem. Lett.* **2010**, *1*, 1590−1594.
(7) Barati Farimani, A.; Aluru, N. R. Spatial Diffusion of Water in Carbon Nanotubes: From Fickian to Ballistic Motion. *J. Phys. Chem. B* **2011**, *115*, 12145−12149.
(8) Han, S.; Choi, M. Y.; Kumar, P.; Stanley, H. E. Phase Transitions in Confined Water Nanofilms. *Nat. Phys.* **2010**, *6*, 685−689.
(9) Barati Farimani, A.; Aluru, N. R. Existence of Multiple Phases of Water at Nanotube Interfaces. *J. Phys. Chem. C* **2016**, *120*, 23763−23771.
(10) Chmiola, J.; Yushin, G.; Gogotsi, Y.; Portet, C.; Simon, P.; Taberna, P. L. Anomalous Increase in Carbon at Pore Sizes Less than 1 Nanometer. *Science* **2006**, *313*, 1760−1763.
(11) Simon, P.; Gogotsi, Y.; Dunn, B. Where Do Batteries End and Supercapacitors Begin? *Science* **2014**, *343*, 1210−1211.
(12) Li, C. P.; Du, M. Role of Solvents in Coordination Supramolecular Systems. *Chem. Commun.* **2011**, *47*, 5958−5972.
(13) Chen, D.; Cui, T. T.; Gao, W.; Jiang, Q. Distinguishing the Structure of High-Pressure Hydrogen with Dielectric Constants. *J. Phys. Chem. Lett.* **2020**, *11*, 664−669.
(14) Schoch, R. B.; Han, J.; Renaud, P. Transport Phenomena in Nanofluidics. *Rev. Mod. Phys.* **2008**, *80*, 839−883.
(15) Faucher, S.; Aluru, N.; Bazant, M. Z.; Blankschtein, D.; Brozena, A. H.; Cumings, J.; Pedro De Souza, J.; Elimelech, M.; Epsztein, R.; Fourkas, J. T.; et al. Critical Knowledge Gaps in Mass Transport through Single-Digit Nanopores: A Review and Perspective. *J. Phys. Chem. C* **2019**, *123*, 21309−21326.
(16) Ahmad, M.; Gu, W.; Geyer, T.; Helms, V. Adhesive Water Networks Facilitate Binding of Protein Interfaces. *Nat. Commun.* **2011**, *2*, 261.
(17) Ballenegger, V.; Hansen, J. P. Dielectric Permittivity Profiles of Confined Polar Fluids. *J. Chem. Phys.* **2005**, *122*, 114711.
(18) Bonthuis, D. J.; Gekle, S.; Netz, R. R. Dielectric Profile of Interfacial Water and Its Effect on Double-Layer Capacitance. *Phys. Rev. Lett.* **2011**, *107*, 166102.
(19) Zhang, C.; Gygi, F.; Galli, G. Strongly Anisotropic Dielectric Relaxation of Water at the Nanoscale. *J. Phys. Chem. Lett.* **2013**, *4*, 2477−2481.
(20) Mondal, S.; Bagchi, B. Water in Carbon Nanotubes: Pronounced Anisotropy in Dielectric Dispersion and Its Microscopic Origin. *J. Phys. Chem. Lett.* **2019**, *10*, 6287−6292.
(21) Bonthuis, D. J.; Gekle, S.; Netz, R. R. Profile of the Static Permittivity Tensor of Water at Interfaces: Consequences for Capacitance, Hydration Interaction and Ion Adsorption. *Langmuir* **2012**, *28*, 7679−7694.
(22) Shannon, M.; Bohn, P.; Elimelech, M.; Georgiadis, J. G.; Mariñas, B. J.; Mayes, A. M. Science and Technology for Water Purification in the Coming Decades. *Nature* **2008**, *452*, 301−310.
(23) Heiranian, M.; Farimani, A. B.; Aluru, N. R. Water Desalination with a Single-Layer MoS 2 Nanopore. *Nat. Commun.* **2015**, *6*, 8616.
(24) Schlaich, A.; Knapp, E. W.; Netz, R. R. Water Dielectric Effects in Planar Confinement. *Phys. Rev. Lett.* **2016**, *117*, 048001.
(25) Fumagalli, L.; Esfandiar, A.; Fabregas, R.; Hu, S.; Ares, P.; Janardanan, A.; Yang, Q.; Radha, B.; Taniguchi, T.; Watanabe, K.; Gomila, G.; Novoselov, K. S.; Geim, A. K. Anomalously Low Dielectric Constant of Confined Water. *Science* **2018**, *360*, 1339−1342.
(26) Motevaselian, M. H.; Aluru, N. R. Universal Reduction in Dielectric Response of Confined Fluids. *ACS Nano* **2020**, *14*, 12761−12770.
(27) Loche, P.; Ayaz, C.; Schlaich, A.; Uematsu, Y.; Netz, R. R. Giant Axial Dielectric Response in Water-Filled Nanotubes an Effective Electrostatic Ion-Ion Interactions from a Tensorial Dielectric Model. *J. Phys. Chem. B* **2019**, *123*, 10850−10857.
(28) Renou, R.; Szymczyk, A.; Maurin, G.; Malfreyt, P.; Ghoufi, A. Superpermittivity of Nanoconfined Water. *J. Chem. Phys.* **2015**, *142*, 184706.
(29) Schaaf, C.; Gekle, S. Spatially Resolved Dielectric Constant of Confined Water and Its Connection to the Non-Local Nature of Bulk Water. *J. Chem. Phys.* **2016**, *145*, 084901.
(30) Qi, W.; Zhao, H. Hydrogen Bond Network in the Hydration Layer of the Water Confined in Nanotubes Increasing the Dielectric Constant Parallel along the Nanotube Axis. *J. Chem. Phys.* **2015**, *143*, 114708.
(31) Abraham, M. J.; Murtola, T.; Schulz, R.; Páll, S.; Smith, J. C.; Hess, B.; Lindah, E. Gromacs: High Performance Molecular Simulations through Multi-Level Parallelism from Laptops to Supercomputers. *SoftwareX* **2015**, *1−2*, 19−25.
(32) Scott, R.; Allen, M. P.; Tildesley, D. J. Computer Simulation of Liquids. *Math. Comput.* **1991**, *57*, 442.
(33) Darden, T.; York, D.; Pedersen, L. Particle Mesh Ewald: An N·log(N) Method for Ewald Sums in Large Systems. *J. Chem. Phys.* **1993**, *98*, 10089−10092.
(34) Yeh, I. C.; Berkowitz, M. L. Ewald Summation for Systems with Slab Geometry. *J. Chem. Phys.* **1999**, *111*, 3155−3162.
(35) Sharma, M.; Resta, R.; Car, R. Dipolar Correlations and the Dielectric Permittivity of Water. *Phys. Rev. Lett.* **2007**, *98*, 247401.
(36) Zhang, C.; Hutter, J.; Sprik, M. Computing the Kirkwood *g*-Factor by Combining Constant Maxwell Electric Field and Electric Displacement Simulations: Application to the Dielectric Constant of Liquid Water. *J. Phys. Chem. Lett.* **2016**, *7*, 2696−2701.
(37) Varghese, S.; Kannam, S. K.; Hansen, J. S.; Sathian, S. P. Effect of Hydrogen Bonds on the Dielectric Properties of Interfacial Water. *Langmuir* **2019**, *35*, 8159−8166.
(38) Muñoz-Santiburcio, D.; Marx, D. Nanoconfinement in Slit Pores Enhances Water Self-Dissociation. *Phys. Rev. Lett.* **2017**, *119*, 056002.
(39) Sirkin, Y. A. P.; Hassanali, A.; Scherlis, D. A. One-Dimensional Confinement Inhibits Water Dissociation in Carbon Nanotubes. *J. Phys. Chem. Lett.* **2018**, *9*, 5029−5033.
(40) Muñoz-Santiburcio, D.; Marx, D. Chemistry in Nanoconfined Water. *Chem. Sci.* **2017**, *8*, 3444−3452.

https://dx.doi.org/10.1021/acs.jpclett.0c03219
J. Phys. Chem. Lett. 2020, 11, 10532−10537